Proceedings of the LHCP2015 Conference, St. Petersburg, Russia, August 31 - September 5, 2015

Editors: V.T. Kim and D.E. Sosnov

Dark Matter Searches at the Large Hadron Collider

ANNAPAOLA DE COSA

Physik Institut, Universität Zürich, Witerthurerstrasse 190, CH-8057 Zürich, Switzerland

annapaola.de.cosa@cern.ch

On behalf of the ATLAS and CMS Collaborations

Abstract. A search for Dark Matter particles directly produced in pair at the Large Hadron Collider is presented. The search is performed using the full LHC Run-I dataset recorded with the CMS and ATLAS detectors in proton-proton collisions at a center-of-mass energy of 8 TeV. Dark Matter production is searched for looking for an excess of events with a large missing transverse momentum in association with energetic light or heavy flavour quark production, or in association with energetic leptons. The search is interpreted within the framework of an effective field theory, as well as of simplified models. No deviation from standard model background expectation is found and exclusion limits on Dark Matter production cross section are obtained.

INTRODUCTION

There is clear evidence of an abundance of matter in the Universe that cannot be explained by the visible matter. This excess, named Dark Matter (DM), accounts for about the 25% of the content of the Universe, while the ordinary matter accounts only for at most 5%. Proof of evidence for Dark Matter comes already in 1970's from the observation of the effects of its gravitational interaction with atomic matter. Despite the overwhelming evidence of the existence of Dark Matter brought to light during the last decades, its nature is still unknown.

Dark Matter is today one of the most compelling indirect evidence for new physics beyond the standard model (SM).

Several theoretical models predict the production of DM at colliders and explain their interaction with SM particles [1][2]. One of the most promising candidates for DM are the Weakly Interactive Massive Particles (WIMPs). Although this is not the unique relevant hypothesis on DM nature, these proceedings will consider only the WIMP-DM models.

The hunt for the WIMPs involves a variety of experiments looking for non-gravitational interaction of DM with SM particles. They can be mainly classified in three categories according to the way in which they look for DM-SM interaction.

- **Direct detection experiments** look for the Dark Matter particle producing recoil energies in the keV energy scale caused by the DM scattering off the target nucleus. Underground experiments look for such kind of signature in the recoil spectrum of single scattering events.
- **Indirect detection experiments** search for products of DM annihilation in dense region of the Universe. DM annihilation is expected to yield standard models particles such as photons and leptons. The predicted branching ratio to different final states depends on the WIMP model assumed. Indirect detection experiments look for an excess in DM-annihilation products.
- **Collider experiments** look for DM pair production in SM particle collisions.

Direct, indirect detection and collider experiments provide complementary approaches to the search for DM as they probe different kinds of WIMP-SM interaction (Fig. 1) in different regions of the phase space.

This paper summarises the results of searches for direct production of Dark Matter at the Large Hadron Collider, LHC, with the CMS (Compact Muon Solenoid) [3] and ATLAS (A Toroidal LHC ApparatuS) [4] experiments, using proton-proton collisions at 8 TeV centre-of-mass energy collisions collected during Run-1.

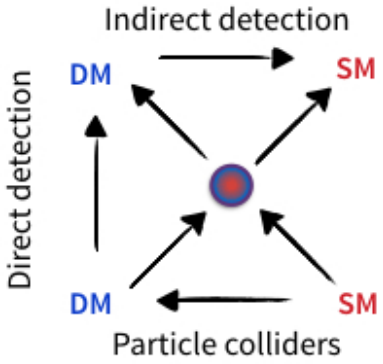

FIGURE 1: View of complementary approach of direct, indirect detection and collider searches to DM-SM interaction.

Searching for Dark Matter at the LHC

If WIMPs produce signal in direct detection experiments, they have to couple to nucleons as well, thus allowing a production of WIMPs in SM-SM collisions. Under this assumption, the large interactions of WIMPs with SM particles implies detectable rates of DM production in the high energy interactions at colliders.

The low DM-mass phase space is particularly suitable for searches at colliders, since a typical collision involving quarks and gluons has a cross section which rapidly falls with the mass of produced states. Therefore, production of light states is favoured, whereas production of massive particles is suppressed.

The WIMP particles are assumed to be stable on collider timescale. This implies a preclusion for the WIMPs to decay within the detector volume: similarly to neutrinos, if produced in SM particle collisions, DM would escape the detector without interacting with it and leaving sign of its passage. Therefore, WIMPs would appear as imbalance of energy in the plane transverse to colliding beams.

Their production can be inferred by measuring the amount of missing energy in the event and looking for the presence of other visible particles recoiling against it. A such clear signature with a high p_T particle and missing energy in the final state is used to flag the interaction and identify it. A rich phenomenology is explored at the LHC looking for Dark Matter, involving final states with energetic jets from light flavour quarks, high p_T leptons as well as jets from heavy flavour quarks.

THEORETICAL APPROACH

Effective Field Theory

Although the nature of the particles mediating the interaction between WIMPs and SM is an essential ingredient to describe the interaction itself, a good simplification can be done in first instance when the mediating particles are heavy compared to the momentum involved in the process. Under this assumption the mediator can be integrated out and the interaction described as contact interaction according to an effective field theory (EFT) approach. Figure 2 shows the diagram pf the DM production in association to a jet from initial state radiation, in the framework of the EFT. While this approach does not provide a complete description of the phenomenology in the whole phase space, still it provides a good approximation for a class of similar models and makes possible a comparison among different kinds of searches in a common framework.

The effective field theory description has also the advantage to be characterised only by three parameters of the theory: the type of interaction between DM and SM (e.g. vector, axial-vector, scalar, pseudoscalar), the mass of the Dark Matter particle, m_χ, and the energy scale of the interaction, often identified as either M^* or Λ, which is related to the mediator mass, M_ϕ, and to the couplings to DM and quarks, g_χ and g_q, by the relation:

$$M^* = \frac{M_\phi}{\sqrt{g_\chi g_q}} \tag{1}$$

The EFT operators were largely employed to interpret results from Run-1 DM searches at the LHC. However, the EFT approach is not a complete theory. It assumes that there are no other new particles accessible at the LHC. It is valid only under the assumption that the momentum transferred in the process is low enough to prevent the mediator to be produced on-shell. At the energies probed at the LHC this may not be the case, and the reliability of the EFT is not guaranteed anymore.

Truncation techniques are exploited to present EFT results. Such techniques consist in rejecting the fraction of events not satisfying the minimum validity requirement for EFT assumption. The transferred momentum is required to be smaller than the mediator mass, $Q_{tr} < M_{\phi}$. This operation weakens the limits leading to less constraining results.

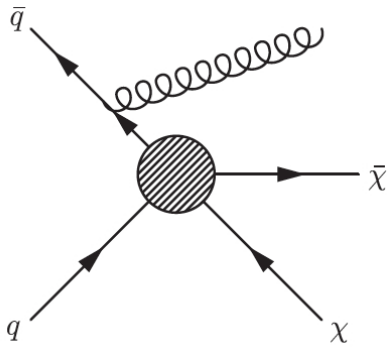

FIGURE 2: Dark Matter production in association with a single jet in the approximation of contact interaction.

Simplified Models

As previously explained, the EFT description holds in cases in which the DM-SM interaction mediator is very heavy compared to the energies involved in the interaction itself. This restricts the phase space that can be covered by this interpretation. Already at the energies reached in Run-1 proton-proton collisions at the LHC, the validity of the assumptions behind the EFT approach is limited. The contact interaction validity issue together with the prospect of much higher energies explored during LHC Run-2 collisions, leads to the need of reconsidering the benchmark models used to interpret the DM searches in Run-1. For cases in which the mediator is not so heavy, or the energy interaction is sufficiently high to produce the mediator on shell, more advanced models are needed that include explicitly the mediator in the theory.

Simplified models are not a complete theory but provide a faithful description of the kinematics of the DM production in the considered processes overcoming the limitations of the EFT approach and giving direct access to the interaction mediator. ATLAS and CMS collaborations, together with the theorist community, have established in September 2014 a forum, the LHC DM Forum, to agree upon the definition of a set of simplified models for the interpretation of results from early Run-2 DM searches. The outcome of this collaboration was summarised in the report of the Forum and made public in July 2015 [5]. An example of simplified model diagrams considered for single-jet plus $\not{E}_T$ signature is shown in Fig. 3. Some of Run-1 searches consider simplified models in addition to EFT for results interpretation in terms of DM production.association

EXPERIMENTAL APPROACH

As anticipated, the production of WIMPs at LHC through the process

$$pp \rightarrow \chi\bar{\chi} \tag{2}$$

is worthless as a discovery mode because it provides no signs for identification of production process. For this reasons processes in which WIMP particles are produced together with additional visible particles radiated off initial partons are considered to infer DM production.

In this way the SM particles are used to flag the interaction and the WIMPs are identified as the missing momentum recoiling against.

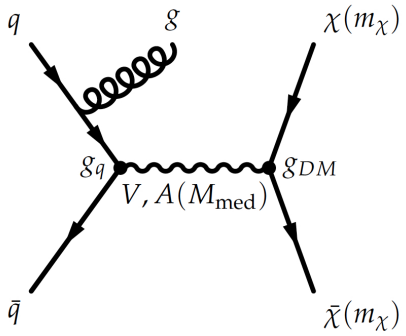

FIGURE 3: Representative Feynman diagram showing the pair production of WIMP particles in association to a single jet from initial state radiation via vector or axial-vector mediator.

Different signatures are exploited for this purpose: WIMPs produced in association with a high transverse momentum jet of hadrons from initial state radiation, or with an energetic electroweak vector boson (γ, W, Z), but also with one or more heavy flavour quarks (top or bottom).

The signature of signal production is an imbalance of energy in the transverse plane, therefore the key variable for all DM searches at LHC is the missing transverse momentum reconstructed in the detector. The main SM physics backgrounds consist of electroweak processes such as the production of Z or W bosons with jets, where the Z decays to neutrinos ($Z \rightarrow \nu\nu$) and the W decays to a neutrino and a charged lepton ($W \rightarrow l\nu$), where the lepton does not fall within the acceptance. Other important source of backgrounds derive from the production of $t\bar{t}$ events producing W bosons and QCD multijet events in which mis-reconstruction of jets leads to fake missing transverse momentum.

To minimize the contribution of non-genuine missing energy from jet mis-measurement and missing energy from non-reconstructed leptons and neutrinos from W or Z decay, specific requirements are applied depending on the signal signature. The selections applied to reject these kinds of backgrounds are described in the next sections together with some sophisticated techniques employed to identify vector boson decays in their low and high momentum regimes.

It is not possible to completely reject background events, thus, a good understanding of the missing transverse momentum distribution for SM backgrounds is essential. The presence of a signal is indeed revealed by an excess of events with respect to the SM background expectation in the high missing transverse momentum region.

To improve the understanding of the background contribution in the tails of high missing transverse momentum, the technique used for the different searches is to define regions enriched in background, called control regions (CRs), and use data distribution in these regions to predict background behaviour in signal region: control-to-signal region transfer factors (TFs) are defined to derive data-driven corrections to background expectation in signal region. A more specific example will be given in the following section for the monojet analysis case.

Monojet searches

Given the high cross section of gluon production from initial state radiation, events with a jet and missing transverse momentum are the most sensitive for most Dark Matter benchmark models proposed. Both ATLAS and CMS have looked for DM production in association with an high-p_T jet [6] [7], events with this signature are also named monojet events. Events selected in this search are required to have one central, high-p_T jet (150/120 GeV in CMS/ATLAS selection) and high $\not{E}_T$ ($\not{E}_T$ >200/150 GeV for CMS/ATLAS). Background events with genuine $\not{E}_T$ from W-decay neutrinos are suppressed by vetoing isolated leptons. Different strategies are employed by ATLAS and CMS to reject multijet events from QCD with non-genuine $\not{E}_T$ du to jet energy mis-measurement. CMS allows a second jet in the event if it is close to the leading one ($\Delta\phi(j_1,j_2)$<2.5), in order to include the frequent cases where initial state radiation yields to two jets. ATLAS allows the presence of even more than two jets, but only if they are produced far from the missing energy ($\Delta\phi(j_i,\not{E}_T)$>1.0).

The dominant backgrounds remaining after the selection described above are $Z \rightarrow \nu\nu + jets$ and $W \rightarrow l\nu + jets$, when the lepton is not reconstructed.

Data-driven techniques are employed to constraint the background in the region where the signal-to-background ratio is high, i.e. in the high missing energy region. A template fit in then performed over the full considered range of

missing energy spectrum.

In order to determine both shape and normalization for the $V + jets$ backgrounds in the signal region, data in background-enriched control samples are defined and used. Control-to-signal region transfer factors are derived as a function of $\not{E}_T$ bins in order to get the background prediction in the signal region applying a correction to data in control regions.

The similarity of Z-decay to neutrinos and to a pair of muons is exploited by defining a dimuon-enriched control sample. The $Z \to \nu\nu + jets$ is hence modelled using the dimuon control region in data. Due to the difference in branching ratio between the two processes (branching ratio of $Z \to \nu\nu$ is about 6 times larger than $Z \to \mu^+\mu^-$ branching ratio), the statistical uncertainty on dimuon template becomes a dominant systematics. A complementary approach used to overcome this issue is to define a regione enriched in $\gamma + jets$ events. The kinematics of this process is very similar to $Z \to \nu\nu + jets$ at large boson transverse momentum. This technique allows to further constrain $Z(\nu\nu) + jets$ background in signal region.

Similarly to what done for Z+jets background, W+jets is corrected by defining a single-muon control region.

The V+jets expectation in signal region is then corrected by performing a simultaneous likelihood fit to the signal and control regions across all the bins. The expected background yields in the i-th bin ($\mu^{Z\to\nu\nu}$ and $\mu^{W\to l\nu}$) in signal region are free parameters of the fit and are constrained from control regions through bin-dependent transfer factors, R_i^V:

$$\mu^{Z\to\nu\nu} = N_i^{Z_{\mu\mu}|\gamma} \cdot R_i^{Z|\gamma} \tag{3}$$

and

$$\mu^{W\to l\nu} = N_i^W \cdot R_i^W, \tag{4}$$

where N_i is the expected number of background events in a given bin i for a specific control region. The transfer factors R_i accounts for differences in signal and control regions for each background process and are derived as the ratio of the number of $Z(\nu\nu) + jets$ events in the signal region to that of $Z(\mu\mu) + jets$ and $\gamma + jets$ events in control regions, or as the ratio of $W(l\nu) + jets$ events in the signal and control region.

The systematic uncertainties are treated as nuisance parameters of the fit, and the transfer factors are allowed to vary within uncertainty.

The pre-fit and post-fit distribution of the $\not{E}_T$ in the signal region for SM backgrounds is shown in Fig. 4 compared to observed $\not{E}_T$ distribution.

The background determination technique described above is adopted by CMS. ATLAS employs a similar procedure to determine background expectation.

Data is found to be in good agreement with SM background expectation from the two experiments: no significant excess is observed in the tails of the distribution. Figure 5 shows the $\not{E}_T$ distribution for background expectation and data as found by the ATLAS experiment.

CMS monojet search does not include multijet events. A dedicated analysis is performed making use of razor variables. The razor variables are used to quantify the transverse imbalance of the jet momenta in events with more jets including b-tagged jets. This category of events gives extra-sensitivity to monojet search, even though the cross section is lower, the di-jet topology provide good discrimination against SM background.

The razor variables employed in this search are defined for dijet events according to the following definition:

$$M_R = \sqrt{(|\vec{p_{J_1}}| + |\vec{p_{J_2}}|)^2 - (p_Z^{J_1} + p_Z^{J_2})^2} \tag{5}$$

and

$$M_T^R = \sqrt{\frac{\not{E}_T(p_T^{J_1} + p_T^{J_2})^2 - \vec{\not{E}}_T \cdot (\vec{p_T}^{J_1} + p_T|\vec{J_2})^2}{2}} \tag{6}$$

where J_1 and J_2 are two mega-jets built from 2 or more jets. These variables were employed to look for the production of invisible particles in cascade decays of heavier particles, and were found to be sensitive to DM direct production as well, as suggested in [8].

Events are classified according to the number of b-tagged jet multiplicity and M_R value. Background expectation is derived from data building single and dimuon categories according to the signal region categorization.

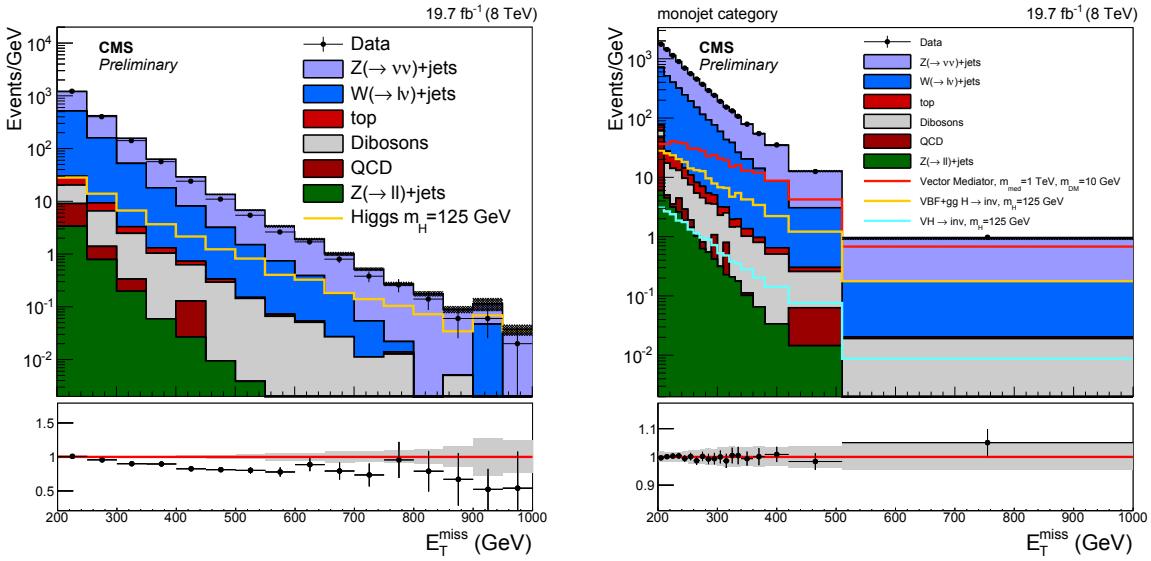

FIGURE 4: Distribution of the $\not{E}_T$ distribution in simulated events (filled coloured histograms) and data (black dots) after the signal selection for the CMS monojet search. Left: Pre-fit distribution. Right: Post-fit distribution. The grey band indicates the statistical uncertainty from MC simulation in the pre-fit plot and the post-fit uncertainty on background in the plot on the right. The expected distribution for a Higgs boson with mass 125 GeV is shown, assuming 100% branching ratio to invisible particles [7].

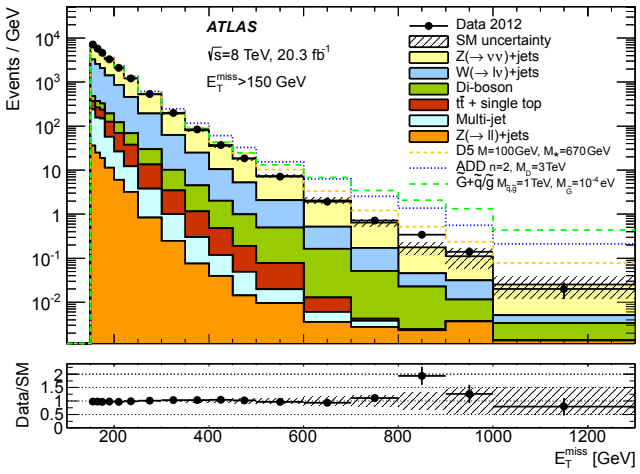

FIGURE 5: Missing transverse momentum distribution for the ATLAS monojet search, showing background expectation (filled coloured histograms) and data (black dots) in the signal region [6].

Figure 6 shows the R^2 distribution for the most sensitive category ($M_R > 600$ GeV). The main systematic uncertainty for this search comes from initial state radiation modelling. No significant excess was observed in this channel.

Mono-V searches

Although the monojet signature is the most sensitive signature for the majority of benchmark models used to interpret the results in terms of DM production, other DM production processes are worth to investigate. Among them signatures with high $\not{E}_T$ and electroweak vector bosons have lower cross section with respect to monojet signature but also

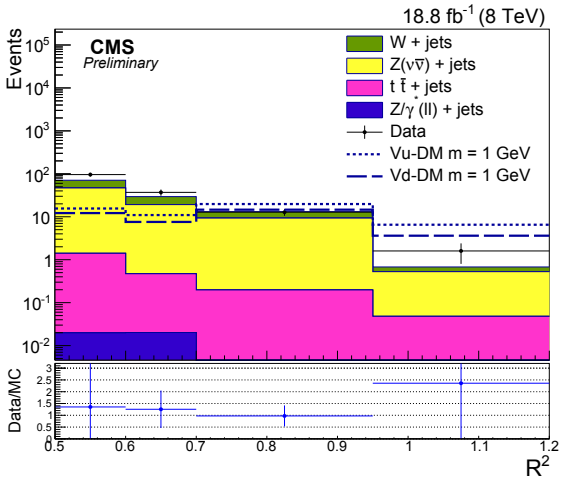

FIGURE 6: Comparison of observed yields and the data-driven prediction in the very high M_R category for the CMS multijet search with razor variables. Background contributions are represented in filled coloured histograms, while data are represented with black dots. Two signal benchmark models are shown, in an EFT model with different vector coupling to up and down quarks [8].

lower background. Mono-W, mono-Z and mono-γ searches are carried out at ATLAS and CMS.

The search for a vector boson recoiling against high $\not{E}_T$ has been performed in both hadronic and leptonic channels. The hadronic channel is quite challenging because of the overwhelming background but it is favoured by the large branching fraction of W and Z boson decay to a pair of quarks, and hence jets. Advanced techniques exploiting informations from the sub-structure of jets are employed to explore mono-V production in the boosted regime. In this region of the phase space the two jets stemmed by the vector boson are produced very close to each other, leading to a unique large jet reconstructed rather than two single jets. Both experiments make use of such techniques to isolate signal-like events from background events.

ATLAS [9] search looks for events with a central, high-p_T, massive jet (*fat jet*) with substructure consistent with two merged jets originated from a W or a Z boson, and with mass consistent with W/Z boson mass. The reconstruction of hadronic V-decay in a fat jet is validated defining a $t\bar{t}$-enriched control region requiring one muon, one fat jet and two additional, well separated narrow jets, out of which at least one b tagged and $\not{E}_T$ >250 GeV. The fat jet mass distribution in the top control region is shown in Fig. 7 comparing predicted backgrounds with data. It is clearly visible the W mass peak and a tail due to the partial or total inclusion of the b jet in the fat jet. The internal structure of a fat jet produced by V decay is characterised by a momentum balance between the two leading subjets, therefore the event is required to satisfy this characteristic in order to reduce background contamination. The momentum balance is defined as:

$$\sqrt{y} = min(p_{T1}P_{T2})\frac{\Delta R}{m_{jet}} \tag{7}$$

and it is required to be larger than 0.4.

Background from SM $t\bar{t}$ events and multijet events is suppressed rejecting events with additional narrow jets not overlapping with the fat jet, or overlapping with the $\not{E}_T$. W + jets background is reduced by vetoing the presence of lepton candidates in the event.

Events are classified in inclusive signal regions with increasing threshold on missing energy: $\not{E}_T > 250$ GeV and $\not{E}_T > 500$ GeV. Similarly to monojet search, the remaining backgrounds arise from $Z \to \nu\nu$ and $W \to l\nu$ production in association with jets, with the latter process begin source of background when the lepton fails identification requirements. These backgrounds are estimated from background-enriched data control regions. Extrapolation factors from control-to-signal region are derived from simulation as a function of m_{jet} and applied to data in control region to get an estimate of expected background in the region of interest.

The fat jet mass distribution in the two $\not{E}_T$ bins in signal region is shown in Fig. 8 for data and expected background as from data-driven prediction.

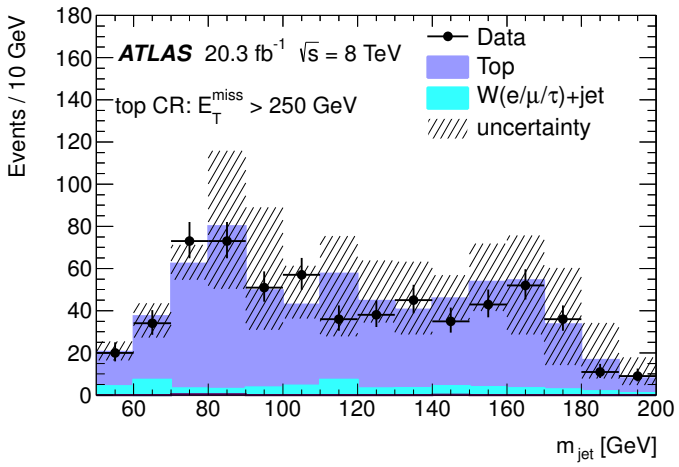

FIGURE 7: Distribution of m_{jet} in the data and for the predicted background in the top control region for the ATLAS search. The region is defined by asking one muon, one fat-jet, two narrow jets and at least one b-tag jet. A requirement on the missing transverse momentum is applied: $\not{E}_T$ >250 GeV. Uncertainties include statistical and systematic sources [9].

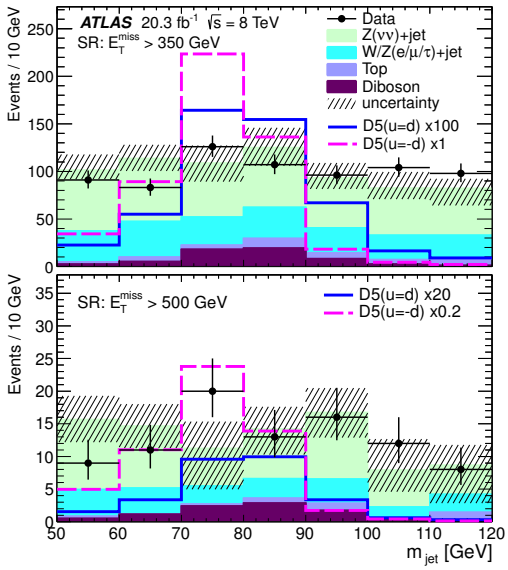

FIGURE 8: Distribution of m_{jet} in the data and for the predicted background in the signal regions with $\not{E}_T$ >350 GeV (top) and $\not{E}_T$ >500 GeV (bottom) for the ATLAS search. Uncertainties include statistical and systematic sources [9].

The major sources of systematic uncertainties affecting the search are due to the limited statistics in the control samples and the theoretical uncertainties in the simulated samples used to derive transfer factors. Uncertainties on jet energy calibration and momentum resolution for the fat jet have also a relevant effect on the final limit.

A fair agreement between data and simulation is observed in the two signal bins defined by different cuts on $\not{E}_T$.

The strategy adopted by CMS [7] differs mainly in the way in which informations on jet substructure are used: CMS looks at how much the fat jet is likely to be originated from 2 quarks using the N-subjettiness [10] variable, τ_N, which quantifies how likely the N-jet structure hypothesis is. The ratio τ_2/τ_1 is a valuable discriminating variable for the boosted-V topology. Figure 9 (left) shows the τ_2/τ_1 distribution in data and simulation.

CMS looks also in the low p_T region of V production to maximise the significance of the search making use

of multivariate techniques to identify the combination of jets originating from V decay. In this regime the two jets stemmed from V-quarks are not merged but rather fully reconstructed. Properties of individual and jets and of di-jet system are exploited to isolate signal-like events.

The mass of the di-jet system is required to be consistent with an weak boson mass ($60 < m_{jj} < 110\ GeV$). The combinatorial background is still dominant after this selection and to resolve the ambiguity picking up the right pair of jets, the multivariate resolved V-tagger is applied.

The V-tagging discriminant is built using as input variables:

- **Quark-Gluon Likelihood Discriminant** value for each jet. This discriminant distinguishes between jets stemmed from quarks and gluons.
- **Jet Pull Angle.** Vector bosons are color-singlet and therefore the two originated quarks are color connected. The color connection of the two jets is exploited looking at the pull angle of the trailing jet with respect to the leading jet and viceversa.
- **Mass Drop.** The mass drop variable is defined from the mass of each jet as well as of the di-jet system and from the distance between the two jets:

$$\frac{\max(m_{j_1}, m_{j_2})}{m_{j_1 j_2}} \Delta R_{j_1 j_2} \tag{8}$$

  This variable is quite helpful in rejecting background given its characteristic to be smaller for dijets from vector boson decay compared to dijets from combinatorial background.
- **Dijet** $p_T(j_1 j_2)/m_{j_1 j_2}$**.** This variable was found to perform nicely against combinatorial background.

The multivariate discriminator defined as described above is used to tag resolved V-tagged events and to choose the best dijet candidate as V candidate. The distribution of the V-tag discriminator is shown in Fig. 9 (right). Events with jets recognised as originating from b are rejected to reduce contamination from top backgrounds.

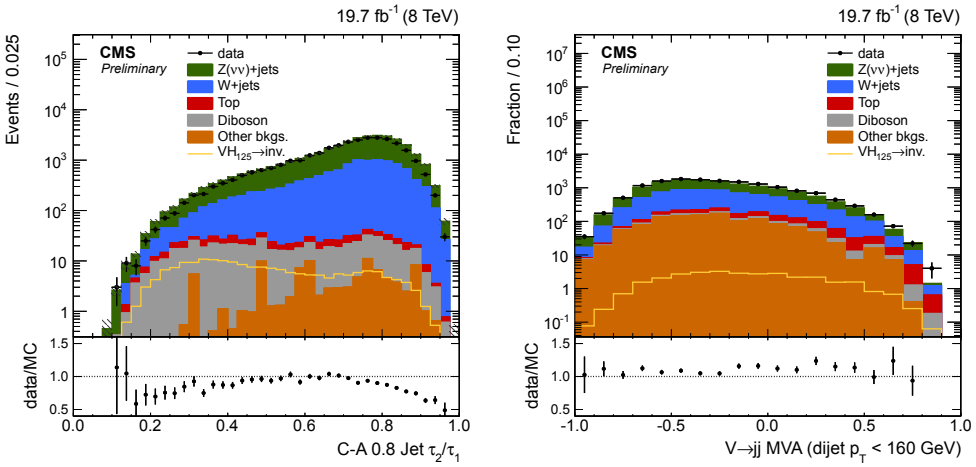

FIGURE 9: Left: Distribution of τ_2/τ_1 variable used in CMS search before the jet mass cut for events in data and MC simulation in the boosted-V event category. Right: CMS resolved V-tagger variable distribution in data is overlaid to expected backgrounds after all other signal region cuts are applied, for dijet p_T <160 GeV [7].

The data-driven strategy adopted by CMS to constraint backgrounds in the signal region for resolved and boosted V + $\not{E}_T$ searches is the same as applied in monojet search.

Data are found to be compatible with SM background expectation and no excess is observed.

Signature with leptonic-decay channels of weak vector bosons are also considered for DM production search. The monolepton search looks for DM pair produced with a W boson radiated off an incoming quark with the W decaying leptonically. Events for this signature are selected if an isolated lepton with $p_T > 100/45$ GeV (electron/muon) [11] is present. A large azimuthal opening angle between the lepton and the $\not{E}_T$ is imposed to discriminate signal from QCD

multijet background. After this selection the major irreducible background is due to $W \rightarrow l\nu$ decay. The W transverse mass, m_T, defined as:

$$m_T = \sqrt{2p_T^l \not{E}_T (1 - cos(\Delta\phi_{l,\not{E}_T}))} \tag{9}$$

has a natural endpoint at M_W, if the $\not{E}_T$ originates only from W neutrino. This is the main discriminating variable against this kind of background. In Fig. 10 (left side), the m_T distribution for SM background expectation and data is shown. ATLAS performs a similar search in this final state [12].

The $Z(ll)+\not{E}_T$ search relies on a clear dilepton signature plus missing energy from WIMP particles. ATLAS search [13] is performed looking for dilepton events with two opposite-sign, same-flavour, isolated leptons, with invariant mass, m_{ll} consistent with M_Z ($76 < m_{ll} < 106$ GeV). The dilepton candidate is required to be produced far from the $\not{E}_T$ in order to reject events where the $\not{E}_T$ originates from mis-reconstructed jets: $\Delta\phi(\not{E}_T, p_T^{ll}) > 2.5$. Top quark background is suppressed by vetoing the presence of reconstructed jets in the event. Similarly events containing a third lepton are removed to reduce diboson background. Nevertheless, the $ZZ \rightarrow l^+l^-\bar{\nu}\nu$ is the dominant background after selection and it is determined from simulation samples. The search looks for an excess of events in the tails of the missing transverse momentum spectrum. Figure 10 (right side) shows distribution of $\not{E}_T$ for data and simulated backgrounds.

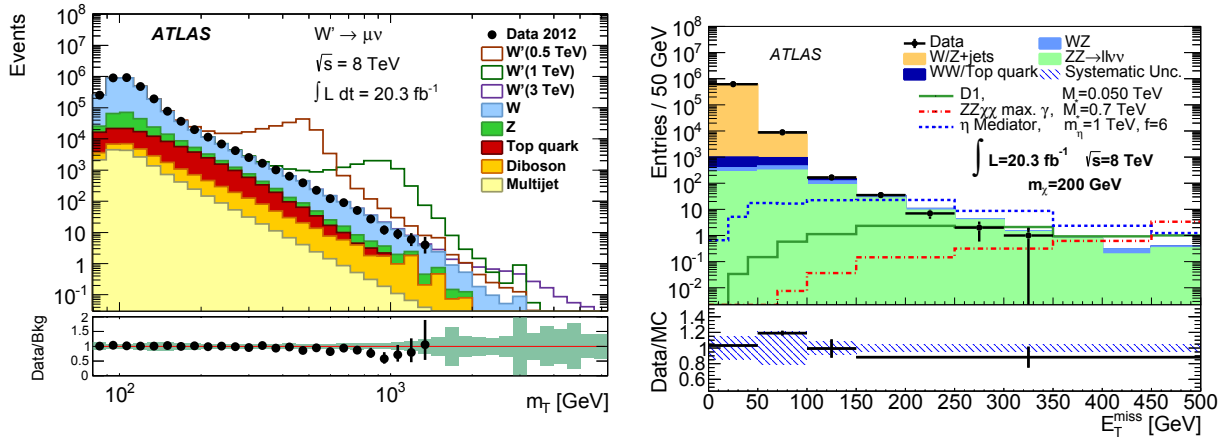

FIGURE 10: Left: Transverse mass spectrum for the muon channel after the event selection of the ATLAS mono-lepton search [12]. Right: missing transverse momentum distribution after all selection for the ATLAS mono-Z search for observed data and background, as estimated from simulation [13].

A similar search is performed by CMS [14], which makes use of the m_T spectrum for the statistical analysis. The m_T variable is defined as:

$$m_T = \sqrt{2p_T^{ll} \not{E}_T (1 - cos(\Delta\phi_{ll,\not{E}_T}))} \tag{10}$$

Signal events are expected to accumulate in the tails. No excess is observed by the two experiments. Data are compatible with the background-only expectation.

Interpretation of Mono-X results

The observations of ATLAS and CMS experiments in the mono-X searches is found to be consistent with background-only hypothesis. Exclusion limits are set on the Dark Matter production cross section and, in the framework of EFT interpretation the limits are translated into lower constraints on the energy scale M^* as a function of the DM mass, for each considered EFT interaction operator. Lower limits on the energy suppression scale are reported in Fig. 11 for the multijet analysis with razor variables. A translation to the DM-nucleon elastic cross section versus Dark Matter mass plane is performed [15] to allow a comparison of LHC results to direct detection experiments.

The 90% CL upper limits on the DM-nucleon scattering cross section for spin independent (vector) and spin dependent (axial vector) interactions is shown in Fig. 12 as a function of the WIMP mass. Comparisons are made with

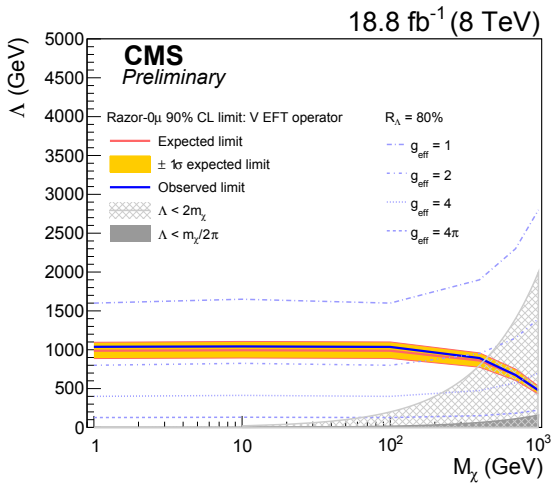

FIGURE 11: Lower limit at 90% CL on the suppression scale M* (Λ) as a function of the WIMP particle mass in the case of vector current. The validity of the EFT is quantified by $R_\Lambda = 80\%$ contours, corresponding to different values of the effective couplings g_{eff} [8].

results from direct detection experiments, showing a complementarity between collider and direct searches. Collider searches are more sensitive at low values of DM mass. This is due to a limitation of direct detection experiments in the low mass region where the recoil signal becomes too soft to be effectively detected. For spin-independent interactions, collider searches provide complementary coverage up to intermediate mass points.

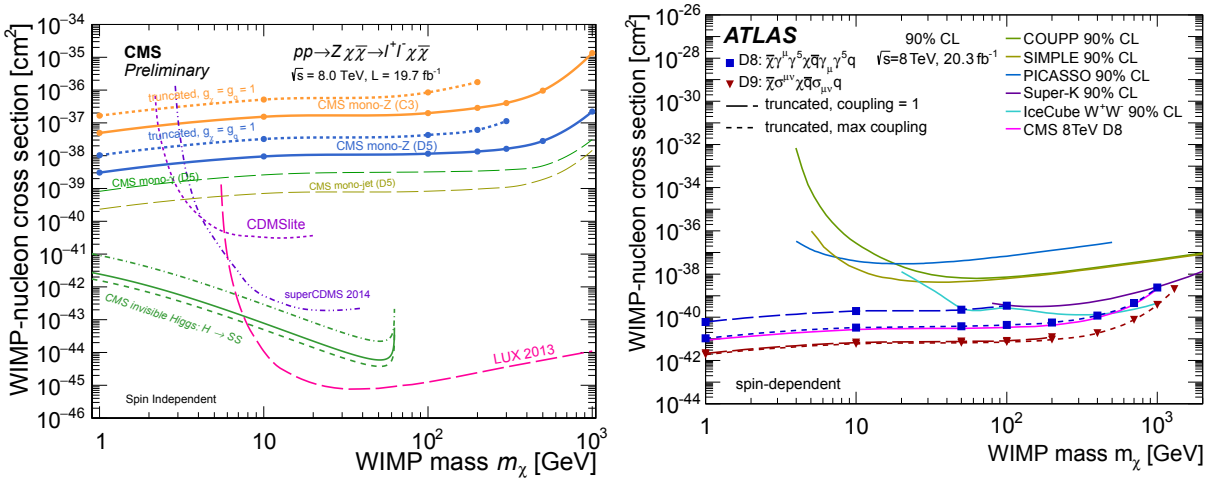

FIGURE 12: Upper limits at 90% CL limit on spin-independent (left) [14] and spin-dependent (right) [6] elastic WIMP-nucleon scattering cross section as a function of DM particle mass for different operators compared to results from direct searches.

The Run-1 results from monojet and monoV analyses are interpreted also in terms of simplified models. In view of 13 TeV LHC collisions, ATLAS and CMS collaborations have established a set of common benchmark simplified models to use for the interpretation of DM search results.

CMS monojet and mono-V searches are interpreted in terms of simplified models following recommendations from the LHC DM Forum.

The mono-V hadronic channel is actually combined with the monojet in CMS search. The events are classified in resolved V-tagged plus $\not{E}_T$, boosted V-tagged plus $\not{E}_T$ and monojet categories, as described above, in order to be orthogonal.

The events fill in the category in cascade, this method assures that the three categories are completely independent.

The 90% CL upper limits are calculated considering the simplified models in terms of exclusion in the $m_\chi - m_\phi$ plane, assuming four different mediators (vector, axial-vector, scalar, pseudo-scalar). The results are summarised in Fig. 13 for vector and axial vector interactions.

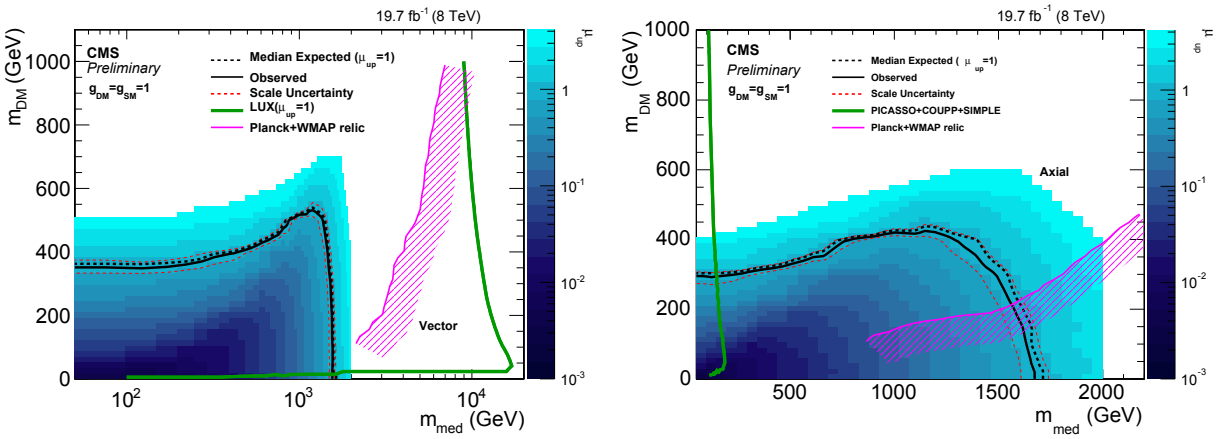

FIGURE 13: Observed 90% CL limits on the signal strength μ, defined as the ratio of the measured cross section to the theoretical cross section, in the $m_\phi - m_\chi$ plane, assuming a vector (left) and axial-vector (right) mediator. A combination of results from monojet, resolved and boosted mono-V categories is used to set limits [7].

DM search in heavy flavour channels

Mono-X searches put stringent bounds on vector interaction, but not on scalar interaction. Coupling to heavy flavour quarks is favoured in case of scalar (pseudoscalar) interaction, given the dependence of the cross section on the mass of quark. Coupling to light flavour quarks is suppressed with respect to top and bottom quarks.

Other Dark Matter searches have been carried out by ATLAS and CMS to further constraint this kind of interactions: final states with missing transverse momentum and a single or a pair of top/bottom quarks have been investigated.

Many models beyond the standard model propose the monotop production in association to an invisible state. Such models can be classified in two categories: resonant and non resonant production. CMS presented results for the monotop production in its hadronic decay channel [16]. ATLAS focused on the signature with a single lepton in the final state [17].

The hadronic channel takes the advantage of the large branching ratio of the top decay to jets. This search looks for events with 3 jets, out of which at least one b tagged, and with invariant mass of the three jets being consistent with the top mass, and large missing transverse momentum. The dominant background comes from V+jets events. The expectation of this process in the signal region is extracted from data in control regions throughout control-to-signal region transfer factors.

Additionally, a lepton veto is applied to suppress backgrounds with genuine $\not{E}_T$ from W decay into leptons.

The semi-leptonic search look for events with exactly one isolated lepton and one b-tagged jet, together with missing energy. The W transverse mass, m_T, and the azimuthal opening angle between the lepton and the b jet are constrained in order to reject background events from multijet QCD with mis-identified leptons and $\not{E}_T$ from jet mis-reconstruction.

The resonant and non-resonant models are partially or totally excluded assuming different values of couplings. Fig. 14 shows the upper limit plot on the invisible state production cross section for the non-resonant model from hadronic channel (left). The resonant model from single lepton channel is excluded in the full mass range for the couplings assumed. In both channels data are found to be compatible with background-only hypothesis. No excess is observed on top of the background expectation and limits on production cross section are set.

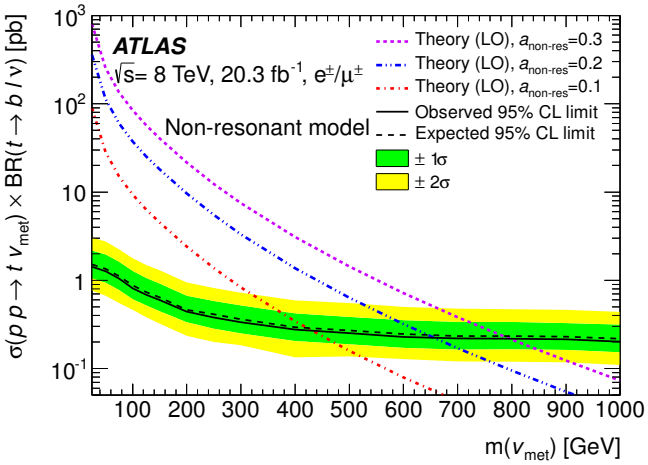

FIGURE 14: Upper limits at 95% CL on monotop production cross section under non-resonant hypothesis. Depending on the assumption on the coupling, states with mass up to 800 GeV are excluded [17].

Beside the monotop search, ATLAS and CMS have searched for a DM pair production in association with a pair of top quarks: ATLAS in the all-hadronic and single-lepton channels [18], while CMS in the semileptonic and dileptonic channels [19][20]. The most sensitive final state is the single-lepton channel, followed by the full hadronic and the dilepton. Events of single lepton topology are identified by requiring exactly one isolated lepton in the event and at least three jets, out of which one identified as b jet. The missing transverse momentum and the pair of leading jets are required to have large azimuthal opening separation, $\Delta\phi(j_{1,2}, \not{E}_T)$, and so to have been produced in different directions, to suppress SM top background. The main backgrounds remaining after the selection are dileptonic $t\bar{t}$ events. These kind of events are rejected applying a requirement on the M_{T2}^W [21]. The contribution from W + jets process is reduced by applying a requirement on the W transverse mass, m_T. The dominant processes, $t\bar{t}$ and W + jets are normalised to data from control regions. A single bin counting experiment is performed in the signal region defined by $\not{E}_T > 350$ GeV and lower limits are placed on the interaction scale at 95% CL for DM-SM scalar interaction (Fig. 15). An analogue search is performed by ATLAS and described in [18]: the $\not{E}_T$ distribution after full selection for the hadronic channel is shown in Fig. 15 (left).

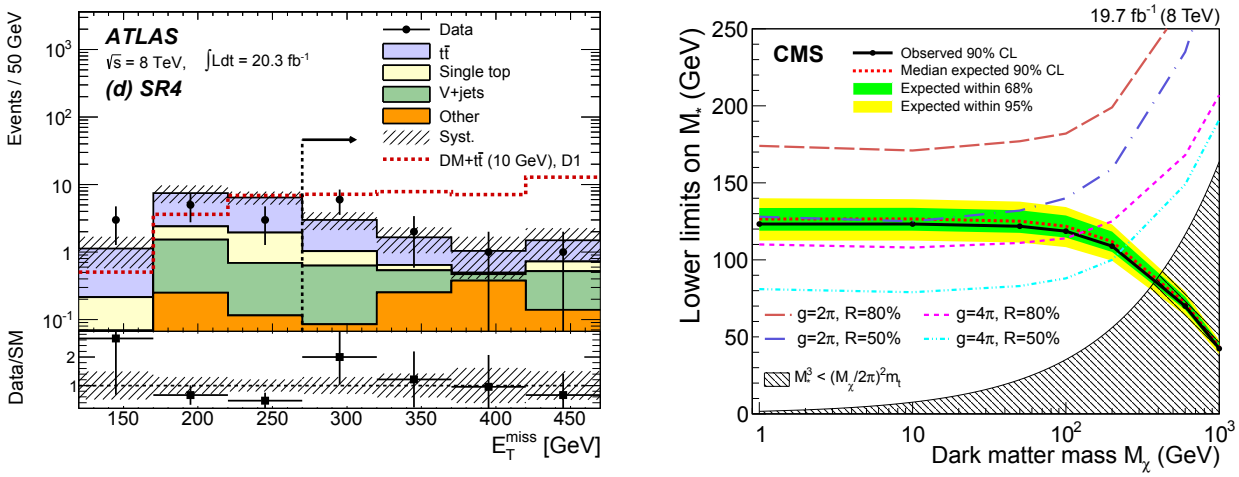

FIGURE 15: Comparison of data and expected SM background for the $\not{E}_T$ distribution in the hadronic channel of ATLAS $t\bar{t} + DM$ search [18], signal for a specific DM scenario is superimposed (left). Lower limits at 90% CL on the interaction scale M^* as a function of WIMP particle mass as resulting from CMS $t\bar{t} + DM$ search [19].

CONCLUSIONS

The ATLAS and CMS Dark Matter searches covered a huge range of final states during the LHC Run-1 data-taking looking for evidence of WIMP particles. The observation is consistente with the SM background expectation in all the channels, and bound have been set on the production cross section considering different models. Results from these searches have been compared to those from direct detection experiments in the framework of an EFT approach. It is clear a complementarity of the two: collider searches are more powerful in constraining the low DM-mass region with respect to direct detection experiments for spin-independent searches where the direct detection suffers a lack of sensitivity. However, the EFT models employed to interpret DM search results, suffer of validity limitation in the high-energy regime. Thus, new models, simplified models, in which the mediator is explicitly considered instead of integrated out, have been employed. These models provide a more fair description of the interaction itself and overcome the limitations of the EFT approach. the simplified models will be the approach followed to interpret the new results coming from LHC Run-2 data taking.

REFERENCES

[1] G. Bertone, D. Hooper, and J. Silk, Phys. Rept. **405**, 279–390 (2005), arXiv:hep-ph/0404175 [hep-ph] .

[2] D. Bauer *et al.* (Snowmass 2013 Cosmic Frontier Working Groups 14), "Dark Matter in the Coming Decade: Complementary Paths to Discovery and Beyond," (2015), pp. 16–23, arXiv:1305.1605 [hep-ph] .

[3] S. Chatrchyan *et al.* (CMS Collaboration), JINST **3**, p. S08004 (2008).

[4] G. Aad *et al.* (ATLAS Collaboration), JINST **3**, p. S08003 (2008).

[5] D. Abercrombie *et al.*, (2015), arXiv:1507.00966 [hep-ex] .

[6] G. Aad *et al.* (ATLAS Collaboration), Eur. Phys. J. **C75**, p. 299 (2015), [Erratum: Eur. Phys. J.C75,no.9,408(2015)], arXiv:1502.01518 [hep-ex] .

[7] V. Khachatryan *et al.* (CMS Collaboration), "Search for New Physics in the V/jet + MET final state," Tech. Rep. CMS-PAS-EXO-12-055 (CERN, Geneva, 2015).

[8] V. Khachatryan *et al.* (CMS Collaboration), "Search for dark matter direct production using razor variables in events with two or more jets in pp collisions at 8 TeV," Tech. Rep. CMS-PAS-EXO-14-004 (CERN, Geneva, 2015).

[9] G. Aad *et al.* (ATLAS Collaboration), Phys. Rev. Lett. **112**, p. 041802 (2014), arXiv:1309.4017 [hep-ex] .

[10] V. Khachatryan *et al.* (CMS Collaboration), "V Tagging Observables and Correlations," Tech. Rep. CMS-PAS-JME-14-002 (CERN, 2014).

[11] V. Khachatryan *et al.* (CMS Collaboration), Phys. Rev. **D91**, p. 092005 (2015), arXiv:1408.2745 [hep-ex] .

[12] G. Aad *et al.* (ATLAS Collaboration), JHEP **09**, p. 037 (2014), arXiv:1407.7494 [hep-ex] .

[13] G. Aad *et al.* (ATLAS Collaboration), Phys. Rev. **D90**, p. 012004 (2014), arXiv:1404.0051 [hep-ex] .

[14] V. Khachatryan *et al.* (CMS Collaboration), (2015), arXiv:1511.09375 [hep-ex] .

[15] Goodman *et al.*, Phys. Rev. **D82**, p. 116010 (2010), arXiv:1008.1783 [hep-ph] .

[16] V. Khachatryan *et al.* (CMS Collaboration), Phys. Rev. Lett. **114**, p. 101801 (2015), arXiv:1410.1149 [hep-ex] .

[17] G. Aad *et al.* (ATLAS Collaboration), Eur. Phys. J. **C75**, p. 79 (2015), arXiv:1410.5404 [hep-ex] .

[18] G. Aad *et al.* (ATLAS Collaboration), Eur. Phys. J. **C75**, p. 92 (2015), arXiv:1410.4031 [hep-ex] .

[19] V. Khachatryan *et al.* (CMS Collaboration), JHEP **06**, p. 121 (2015), arXiv:1504.03198 [hep-ex] .

[20] V. Khachatryan *et al.* (CMS Collaboration), "Search for the Production of Dark Matter in Association with Top Quark Pairs in the Di-lepton Final State in pp collisions at $\sqrt{s} = 8$ TeV," Tech. Rep. CMS-PAS-B2G-13-004 (2014).

[21] C. G. Lester and D. J. Summers, Phys. Lett. **B463**, 99–103 (1999), arXiv:hep-ph/9906349 [hep-ph] .

[22] G. Aad *et al.* (ATLAS Collaboration), "Search for dark matter pair production in events with a hadronically decaying W or Z boson and missing transverse momentum in pp collision data at $\sqrt{s} = 8$ TeV with the ATLAS detector," Tech. Rep. ATLAS-CONF-2013-073 (CERN, 2013).

[23] N. F. Bell, Y. Cai, J. B. Dent, R. K. Leane, and T. J. Weiler, Phys. Rev. **D92**, p. 053008 (2015), arXiv:1503.07874 [hep-ph] .